

# Integration of Small Cells with Smart Antennas in Macrocells for Improving the Performance of Mobile Telephone Networks

Alphonse Binele Abana<sup>1</sup>, Patrick Dany Bavoua Kenfack<sup>1</sup>, Emmanuel Tonye<sup>1</sup> & Claude Francine Onana Nomo<sup>1</sup>

<sup>1</sup> Department of Electrical and Telecommunications Engineering, National Advanced School of Engineering of Yaounde, University of Yaounde I, Yaounde, Cameroon

Correspondence: Patrick Dany Bavoua Kenfack, Department of Electrical and Telecommunications Engineering, National Advanced School of engineering of Yaounde, University of Yaounde I, Yaounde, Cameroon. Tel: (+237)-69-966-7134. E-mail: danybavoua@gmail.com

Received: April 16, 2023 Accepted: May 20, 2023 Online Published: June 1, 2023

doi:10.5539/nct.v8n1p8

URL: <https://doi.org/10.5539/nct.v8n1p8>

## Abstract

In macrocellular networks, there are areas where it is difficult to have satisfactory connectivity. In practice, the delays for sending or downloading multimedia applications, or even consulting web applications can become quite long.

One solution is to deploy cells with smaller ranges called small cells inside the macrocell, closer to subscribers in order to boost network capacity. Only, with the instability of electrical energy, the small cells may not be powered properly. A way should therefore be found to further reduce the energy consumption of small cells in order to facilitate their deployment in Cameroon. To do this, we opted for the solution of smart antennas to be integrated into the small cells; antennas that transmit at the request of users and according to their needs.

In this work, we design and build an application that illustrates the performance of small cells with three key innovations:

- Smart antennas make it possible to estimate users' directions and deliver a maximum radiation pattern in those directions, while minimizing interference.
- The capacity of a heterogeneous network is boosted compared to that of a homogeneous network.
- The signal attenuation in free space in a micro cell is a function of the user-small cell distance. The application that we propose is therefore a relevant decision-making tool for the engineering and planning of mobile networks

**Keywords:** macrocell, small cell, capacitance, smart antenna, attenuation

## 1. Introduction

The technological evolution in mobile telephony, marked recently by the arrival of 5G in mid-2019 (<https://www.google.com/amp/s/www.lesechos.fr/amp/1357263>) and 6G announced for the year 2030 (Par Ando, 2021), has prompted many countries to acquire these technologies to be in the era of time. Their major advantage is in particular connection speeds of the order of Gigabits for 5G and Terabits for 6G. However, some countries in general and Cameroon in particular are only covered up to 4G technology. However, with technological and demographic evolution and increasing urbanization, connection speeds are slow, leading to dissatisfaction among subscribers. To reduce this inconvenience, one solution is to deploy small cells, which are mini base stations, as close as possible to subscribers. These small cells offer mobile telecommunications operators the possibility of increasing the capacity of existing wireless networks (Contrôles Essais Mesures, 2022). However, the classic small cells permanently radiating consume more electrical energy, we propose as a solution to integrate smart antennas into the small cells. The latter consume less energy because they radiate in a timely manner in privileged directions while minimizing interference. We have, as part of this work, designed and produced an application to highlight the performance of small cells.

## 2. Integration of Small Cells to Increase the Performance of Mobile Networks

### 2.1 Telecommunications Site

A telecommunications site is the set consisting of a telecommunications tower or small cell and energy equipment to power the various equipment located there. Thus, we will speak of a macro site for a site with a telecommunications tower and a microsite for a site with a small cell.

#### 2.1.1 Homogeneous Network (Macro-Network)

A telephone network is a set of interconnected cells. A homogeneous network or macro-network is a telephone network made up 100% of telecommunications towers.

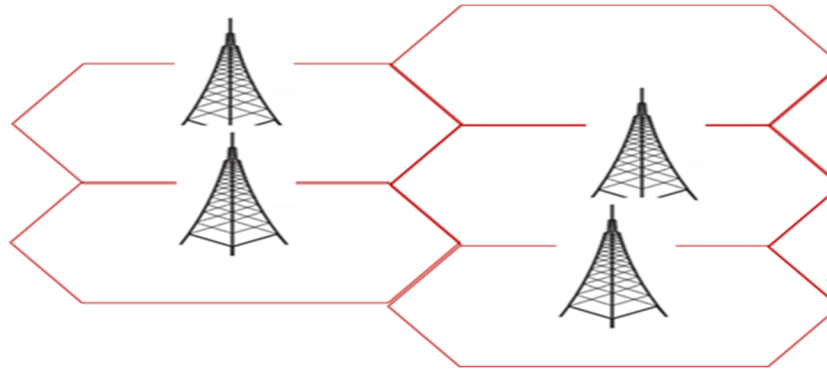


Figure 1. Homogeneous network (<https://blogs.univ-poitiers.fr/f-launay/files/2021/01/figure11.png>)

#### 2.1.2 Heterogeneous Network

A heterogeneous network is a network made up of both macrocells and small cells.

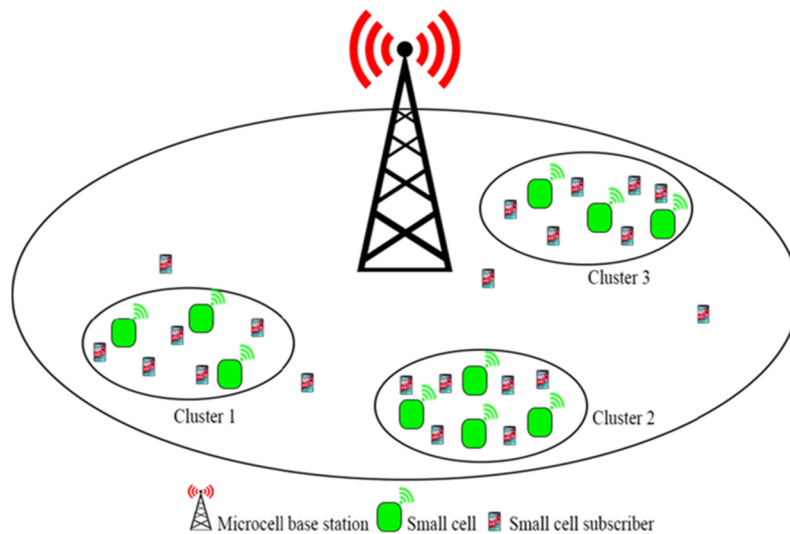


Figure 2. Heterogeneous network

(<https://www.researchgate.net/profile/Subha-Ghosh/publication/337432350/figure/fig1/AS:962228639510561@1606424593740/Small-cell-clustering-under-microcell-base-station.png>)

Caption: In Figure 2, the green drawings represent macrocells and the purple drawings represent small cells.

## 2.2 Impact of Small Cells on Mobile Network Capacity

### 2.2.1 Technological Constraints

Given the technological advances in the world, telecommunication towers no longer being sufficient to ensure satisfactory coverage and capacity, the concept of “small cells” was therefore developed to overcome these shortcomings.

Indeed, with a network consisting exclusively of macro cells, there is a low capacity of the network materialized by slow, or even very slow, connection speeds.

In addition to the coverage hole problem solved by small cells, it has been noticed that high data rates are generally possible when subscribers are very close to the antenna.



Figure 3. Increase in throughput approaching base stations (GSM Association, 2016)

Small cells are therefore designed to supplement the macrocell in one of its tasks, which is to provide correct connectivity to subscribers, characterized by high speeds. Thus, in a heterogeneous network, the network capacity is significantly boosted. The small cells are connected to the macro cells by a backhaul link which can be: optical fiber or microwave links.

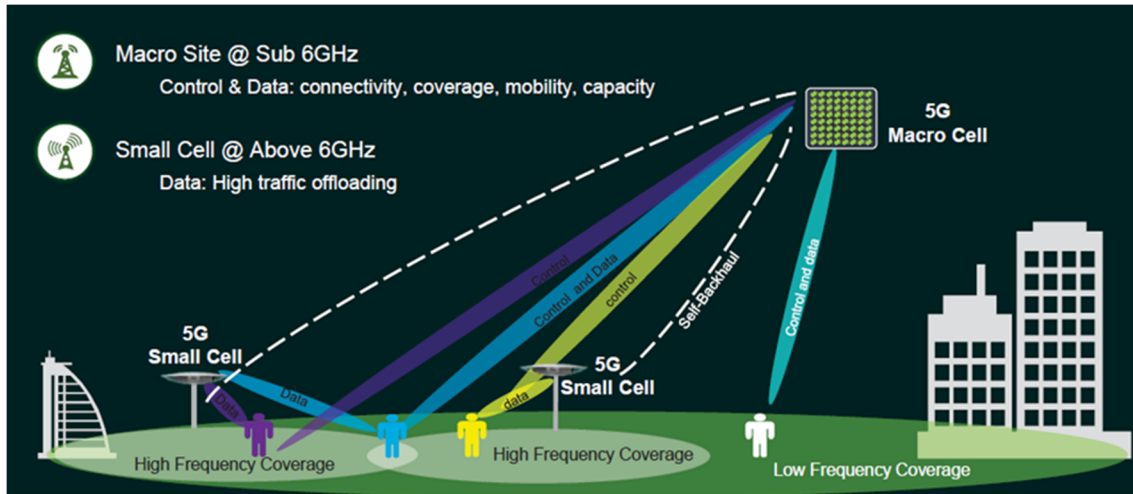


Figure 4. Example of heterogeneous network in 5G with boosted capacity (Issakov, 2016)

Three main exogenous phenomena contribute to the degradation of capacity in mobile networks: demographic explosion, technological evolution, increasing urbanization

### 2.2.2 Network densification through capacity

As explained above, in a homogeneous network, the capacity is considerably reduced due to various factors such as technological evolution, demographic explosion and increasing urbanization.

With demand for capacity growing exponentially year on year, mobile operators need to find a way to increase network capacity without increasing connection charges to satisfy their subscribers. In this part, from the capacity formula given in (Shannon, 1949) by Shannon, we will explore in turn the different ways to increase the capacity of a telephone network and show that the deployment of small cells is the solution. the most effective.

$$C = B \log_2(1 + SINR)$$

From the capacity formula, one can get an insight into the factors influencing the capacity in a network. Thus, we have:

- The B bandwidth

It represents the width of the channel through which the data passes. In a pictorial and simplified way, considering a water pipeline, the speed at which the water flows in the channel is considered as the capacity or the flow rate; while the channel in which the water flows is considered as the bandwidth. 4G band plans represent between 5 MHz and 20 MHz of bandwidth per channel, while the 5G FR1 standard allows between 5 MHz and 100 MHz of bandwidth per channel (Shannon, 1949). Thus, the bandwidth being proportional to the capacity, to increase the capacity of a network, one could decide to increase the bandwidth. Unfortunately, this solution is not the most obvious because the bandwidths are allocated by the ITU to the operators and therefore do not depend on them.

- The SINR ratio whose formula is:  $SINR = \frac{Signal}{Interference+Bruit}$  (2)

To increase the capacity, one could also choose to increase the SINR. To do this, it would be necessary to reduce interference and noise. Increasing the SINR is equivalent to improving the spectral efficiency; this can be done using different modulation techniques. This solution is not very efficient either, because the SINR is inside a logarithmic function which does not grow rapidly.

The third solution is to reduce the size of the cells. This implies that in a macrocell, a few small cells are deployed which will make it possible to route the traffic of the macrocell as close as possible to the subscribers, in order firstly to circumvent urban obstacles and secondly to boost the capacity of the network.

An overview is given in the study conducted in (Webb, 2007); study that highlights capacity gains between 1950 and 2000 using the above three methods:

- The capacity is boosted by 2700× by deploying the small cells.
- Capacity is 15× higher by increasing bandwidth
- The capacity is 10× improved by increasing the SINR by modulation, coding techniques.

### 2.2.3. Signal attenuation in free space in an urban environment

During the propagation of electromagnetic waves, these are attenuated. What actually causes this attenuation are obstacles. If the signal was transmitted from a starting point A to an ending point B without any obstacle, it would be returned with almost the same power at point B. With urban development in particular, these obstacles are mainly buildings (hotels, businesses, restaurants, etc.). These barriers prevent users from being fully covered by the network. It is possible to evaluate the free space attenuation of the signal by the FRIIS formula:

$$A = \left(\frac{4\pi d}{\lambda}\right)^2 = \left(\frac{4\pi d f}{c}\right)^2 \quad (3)$$

Where f represents the frequency in Hz, c the speed of light in vacuum in m/s.

$$\begin{aligned} A_{dB} &= 2 \times 10 \log\left(\frac{4\pi d f}{c}\right) \\ A_{dB} &= 20 \log\left(\frac{4\pi \times (d \times 10^3) \times (f \times 10^6)}{c}\right) \\ A_{dB} &= 20 \log\left(\frac{4\pi \times 10^9}{c}\right) + 20 \log(f_{MHz}) + 20 \log(d_{km}) \\ A_{dB} &= 32,45 + 20 \log(f_{MHz}) + 20 \log(d_{km}) \end{aligned} \quad (4)$$

After breaking up macro cells into small cells, as subscribers are now closer to base stations, signal attenuation will be less.

Thus, in a heterogeneous network, the free space attenuation formula is not the same as in a homogeneous network. It will be evaluated in two stages: first the attenuation in the LOS area and the attenuation in the NLOS area. The LOS zone designates the zone of direct visibility between the user and the base station, i.e. without any obstacle to the signal. On the contrary, the NLOS area corresponds to the area of direct “no visibility” between a user and a base station.

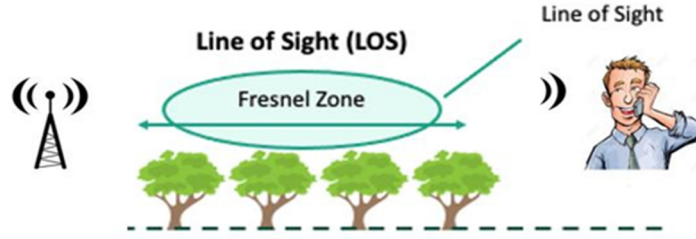


Figure 5. Zone LOS

(<https://cdn.sketchbubble.com/pub/media/catalog/product/optimized1/a/9/a9c208093dc77b45f6c3518a311fac25167e840ef765f526f567b06184fd69f8/line-of-sight-model-mc-slide1.png>) (modifiée par l'auteur)

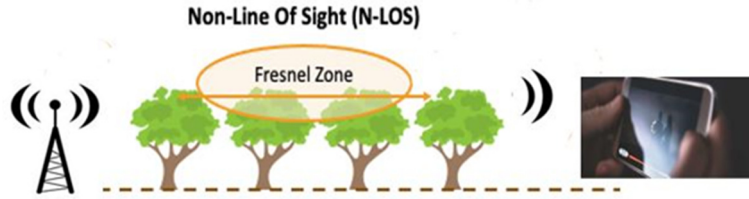


Figure 6. NLOS area

(<https://cdn.sketchbubble.com/pub/media/catalog/product/optimized1/a/9/a9c208093dc77b45f6c3518a311fac25167e840ef765f526f567b06184fd69f8/line-of-sight-model-mc-slide1.png>) (modified by author)

The free space and urban attenuation in a heterogeneous network is given by the set of formulas in (Claussen et al., 2017):

$$\begin{cases} G_{LOS_{dB}} = -22 \log(d_{mètres}) - 20 \log(f_{GHz}) - 28 \\ G_{NLOS_{dB}} = -36,7 \log(d_{mètres}) - 26 \log(f_{GHz}) - 22,7 \\ p_{LOS} = \min\left(\frac{18}{d}, 1\right) \times \left(1 - e^{-\frac{d}{36}}\right) + e^{-\frac{d}{36}} \\ G_{dB} = p_{LOS} \times G_{LOS_{dB}} + (1 - p_{LOS}) \times G_{NLOS_{dB}} \end{cases} \quad (5)$$

Where  $d$  represents the distance between the user and the microcell  $f$  represents the frequency of the signal.

### 3. Smart Antennas and Algorithms Used

#### 3.1 Smart Antennas

To have smart antennas, there are algorithms to be integrated into a DSP (Digital Signal Processing). The DSP is the brain capable of manipulating the electrical signals coming from the antenna. In order to better understand the concept of smart antenna, also called adaptive antenna, it is necessary to understand the difference with a conventional antenna. The main characteristic of a conventional antenna is that it radiates like a lamppost, 24/7 (the position of the user being unknown), whether there are users requesting it or not.



Figure 6. Principle of a classic antenna

(<https://cdn.sketchbubble.com/pub/media/catalog/product/optimized1/a/9/a9c208093dc77b45f6c3518a311fac25167e840ef765f526f567b06184fd69f8/line-of-sight-model-mc-slide1.png>)

In addition, with the conventional antenna, the signal is emitted regardless of the users' needs. So, in this scenario, it is possible that the signal is served in an area where users have not wanted to use it and that where the need is, the signal strength is not high enough to satisfy subscribers. .

In addition, while a conventional antenna broadcasts personal conversations in all directions, the smart antenna precisely detects the position of users and delivers signals only in their direction. Thus, it can optimize the reception of a communication from a mobile, while minimizing interference with any signals from other telecommunications.

The smart antenna, on the other hand, does not continuously emit the signal but only when it is requested by a user. In this case, the signal delivered by the antenna is directed according to the position of the users; it is adapted to their mobility and their needs, as shown in Figures 7 and 8.

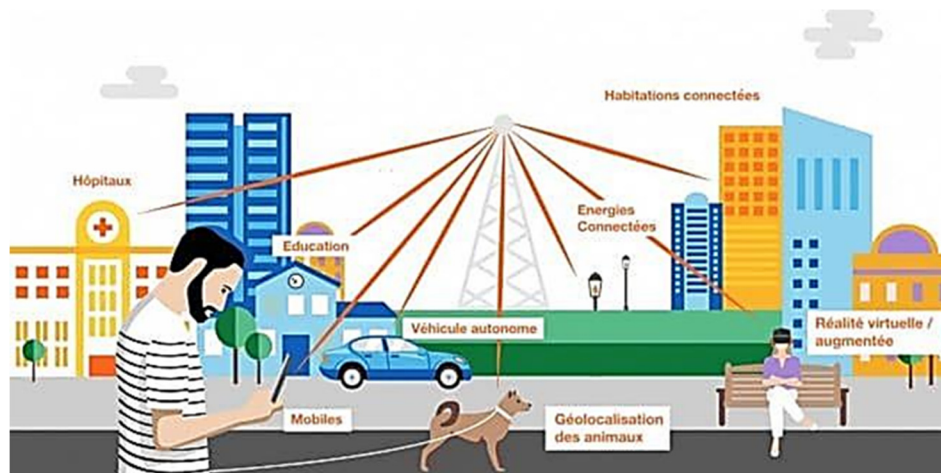


Figure 7. Principle of a smart antenna (Les bénéfices de la 5G, 2022)

The mechanisms used by smart antennas are:

- The formation of beams (in English: beamforming) which consists in emitting the signal at the request of the user and in the direction of this one.
- Beam tracking (in English: beamtracking) which consists of ensuring beam tracking when the user is moving.

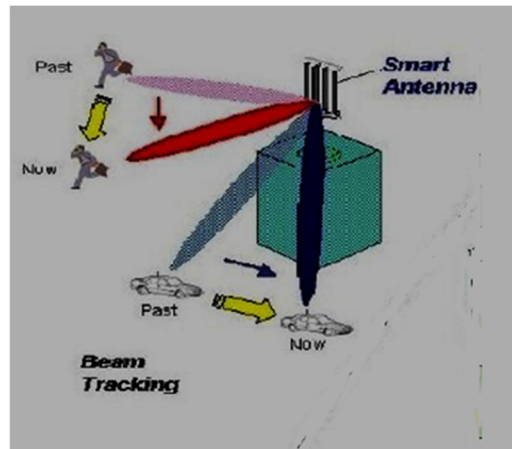


Figure 8. Principle of beamtracking (Les bénéfices de la 5G, 2022)

- Data slicing, which consists of adapting the power of the signal delivered to the needs of the user. Simply put, data slicing is network virtualization. That is to say that the network is cut into slices and each slice is configurable according to the use it supports. This enables real-time, à la carte network management. This also makes it possible to prioritize uses (Tout savoir sur les antennes 5G, 2022). For example, the power delivered to a user who wishes to write an SMS will be significantly lower than that delivered to a user who wishes to download an application.

To do this, the adaptive antenna integrates two types of algorithms embedded in a DSP in order to optimize the management and distribution of the signal to users. The two algorithms in a successive and ordered way are:

- The DDA estimation algorithm

Its purpose is to estimate the directions of arrival of signals from users. This allows the smart antenna to know the different positions of the users.

- The beamforming algorithm

This algorithm aims to modify the radiation pattern of the antenna. The latter consists of a main lobe (yellow and red colors) and secondary lobes (green and blue colors) as shown in Figure 9.

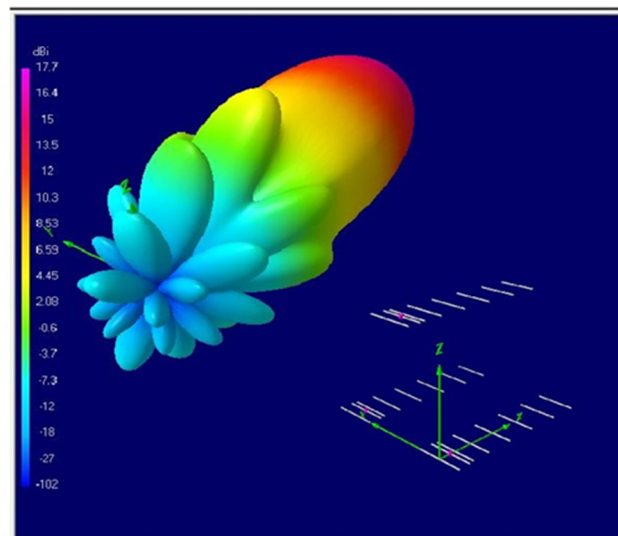


Figure 9: 3D radiation pattern of an antenna

(<https://encrypted-tbn0.gstatic.com/images?q=tbn:AND9GcQuL-DMFyYtCpOrGRTOLkYNP0ckLeCqx36-5g&usqp=CAU>)



The main lobe is the maximum power signal that is directed towards the user. Side lobes are signals of low power, or even lower power than the main lobe, representing interfering users (which may or may not come from the same cell). The aim of the beamforming algorithm is therefore to form the beams in the directions of the users on the one hand, while minimizing the interference (tending the powers of the secondary lobes towards zero) in order to improve the quality of the signal d 'somewhere else. In doing so, it helps to boost the capacity of the network and therefore to have a high throughput per user and thereby satisfy network users.

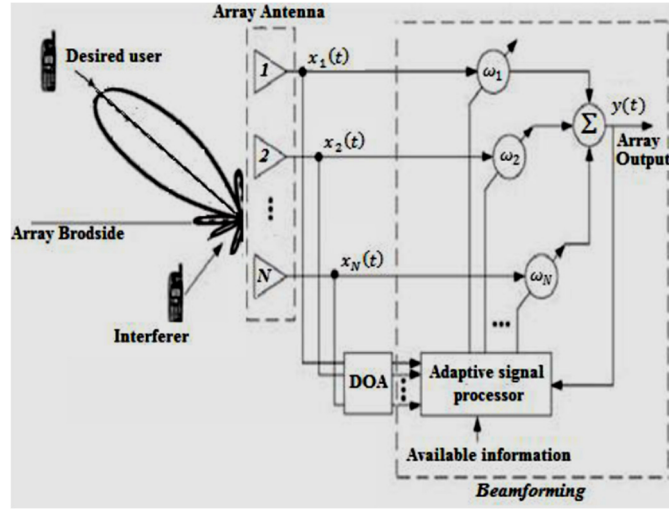


Figure 10. Block diagram of a smart antenna system (Naceur & Merahi, 2012)

In Figure 10, the first block of the system (DOA) aims to determine the angle of arrival of the incident signals on the radiating elements constituting the antenna. With beamforming algorithms, these DDA estimation algorithms will be integrated into a DSP in order to have an adapted radiation pattern output, that is to say whose maximum power is in the direction of the user and minimal in the directions of the interferents.

### 3.2 Algorithms Used

#### 3.2.1 DDA Estimation Algorithms

Most of the information that will be provided regarding DDA estimation algorithms is taken from (Tonye & Kepchabe, 2023).

In (Kamil, Ismail, & Bashar, 2021), or a network of  $M$  radiating elements on which arrive signals from  $D$  different directions  $\theta_1, \theta_2, \theta_3, \dots, \theta_D$ . The signals received are then noisy linear combinations of the source signals as shown in Figure 11.

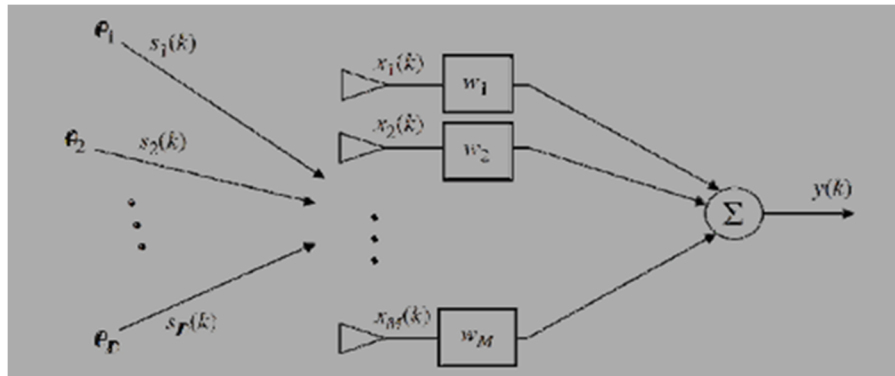


Figure 11. Signals arriving on an array of radiating elements (Kamil, Ismail, & Bashar, 2021)

By performing  $L$  observations, the reception vector at the output of the array of radiating elements is written:



$$x(t) = A(\theta).s(t) + n(t). \quad (6)$$

où  $A(\theta) = [a(\theta_1) a(\theta_2) \dots a(\theta_M)]$  . is the matrix of directional vectors of the sources; it contains information on the angles of arrival.

$s(t) = [s_1(t), s_2(t), \dots, s_D(t)]^T$  is the vector of the complex envelopes of the D sources.

$n(t)$  is the Gaussian additive noise.

The covariance matrix  $R_{xx}$  for an observation is given by:

$$R_{xx} = E\{x(t)x^H(t)\} \quad (7)$$

$$R_{xx} = AE\{s(t)s^H(t)\}A^H + E\{n(t)n^H(t)\} \quad (8)$$

$$R_{xx} = AR_{ss}A^H + \sigma^2 I$$

Where  $\sigma^2 I$  is the noise covariance matrix with  $\sigma^2$ , noise power for each element of the network and I the identity matrix,  $R_{ss}$  is the covariance matrix of the signal vector and H is the Hermitian.

The estimated covariance or correlation matrix  $\hat{R}$  for L observations is given by:

$$\hat{R} = \frac{1}{L} \sum_{k=1}^L x(k)x(k)^H \quad (9)$$

From the correlation matrix and according to the different DDA estimation algorithms, the power of the spatial spectrum is determined. The angles of arrival of the signals will be estimated by looking for the maximum values of this spectrum.

Subscriber sourced DDA estimation algorithms can be grouped into two categories:

#### 3.2.1.1 Spectral Estimation Methods

##### ▪ **Bartlett algorithm**

BARTLETT's method is based on the spatial Fourier transform. Indeed, it is one of the first methods used to detect angles of arrival. Its principle is widely developed there. The latter is to perform the Fourier transform in the space of the received signals. If we plot this function for a given wave, we obtain an energy peak for the direction in which the source is located. Its pseudo-energy spectrum is given by:

$$P_B = \frac{1}{M^2} A^H R_{xx} A \quad (10)$$

##### ▪ **Prony Algorithm**

Also called "linear prediction method", this algorithm was developed by Prony in 1795. Its principle is to minimize the prediction error on the response of any element of the network. Finding the weighting coefficients responsible for minimizing the average value of this error leads to the pseudo-spectrum:

$$P_P = \frac{U_m^H R_{xx}^{-1} U_m}{|U_m^H R_{xx}^{-1} A|^2} \quad (11)$$

Where  $U_m$  is the mth column of the identity matrix  $I_M$ .

##### ▪ **Capon Algorithm**

This algorithm was developed by Capon in 1969. It is based on an unbiased estimation with minimum variance (MVDR: Minimum Variance Distortionless Response). Its pseudo-spectrum is determined by:

$$P_C = \frac{1}{A^H R_{xx}^{-1} A} \quad (12)$$

##### ▪ **MEM Algorithm (Maximum Entropy Method)**

This method makes it possible to find a power spectrum such that its Fourier transform is equal to the measured correlation on the condition that its entropy is maximized. The solution to this problem requires the search for infinite dimension, which can be transformed into finite dimension using the principle of duality. We obtain :

#### 3.2.1.2 Structural eigenvalue methods (or subspace method)

##### ▪ **Pisarenko Algorithm (MMSE)**

Its purpose is to minimize the root mean square error at the output of the network under the constraint that the norm of the vector of the weight is equal to unity. Its pseudo-spectrum is:

$$P_{MMSE} = \frac{1}{|A^H e_1|} \quad (13)$$

where  $e_1$  est le vecteur propre associé à la valeur propre  $\lambda_1$ .

#### ▪ **MUSIC Algorithm**

This approach was approached by Schmidt in 1979. It is based on the decomposition of the space of the signals delivered into a signal subspace and a noise subspace.

Indeed, in (Mubeen, Prasad, & Rani, 2012), once the autocorrelation matrix is known, the different steps leading to the detection of the angles of arrival are as follows:

- Calculation of eigenvectors and eigenvalues of the autocorrelation matrix  $R_{xx}$ .
- Classification of these eigenvalues according to decreasing values and identification of the eigenvectors associated with the most important eigenvalues: these vectors constitute a basis of the signal subspace. The remaining eigenvectors form a basis for the noise subspace.
- Construction of a family of vectors parametrized by the angle of arrival having a theoretical relative phase state imposed by the geometry of the network.
- Projection of this family of vectors on the noise subspace and determination of the values of the direction of arrival for which there is a relative minimum.

The spatial spectrum power of the MUSIC algorithm is given by:

$$P_{MUSIC} = \frac{A^H A}{A^H E_n E_n^H A} \quad (14)$$

#### ▪ **ESPRIT Algorithm**

Here, the array of radiating elements is decomposed into two sub-arrays X and Y shifted by. The signal received on the second sub-network is then out of phase with respect to the first. From these two sub-networks, we will obtain two correlation matrices  $R_X$  and  $R_Y$  from which we can derive eigenvalues. Then, we look for the matrix  $\Psi$  to pass from one to the other. We then deduce the angles of arrival of the signals by:

$$P_E = \arccos \frac{[\arg(\lambda_1)]}{2\pi\Delta} \quad (15)$$

Où  $l = 1, \dots, L$  et  $\lambda_l$  the eigenvalues of  $\Psi$ .

#### **MIN-NORM Algorithm**

Developed by REDDI, KUMARESAN and TUFS, this algorithm optimizes the weight vector by solving the system of equations:

$$\begin{cases} \min(W^H W) \\ E_S^H W = 0 \\ W \cdot e_1 = 1 \end{cases} \quad (16)$$

Where W is the matrix of weights of dimension  $M \times M$ .

The solution leads to the pseudo-spectrum:

$$P_{MN} = \frac{1}{|A^H E_b E_b^H e_1|^2} \quad (17)$$

Figure 12 presents the titles of the different DDA estimation algorithms.

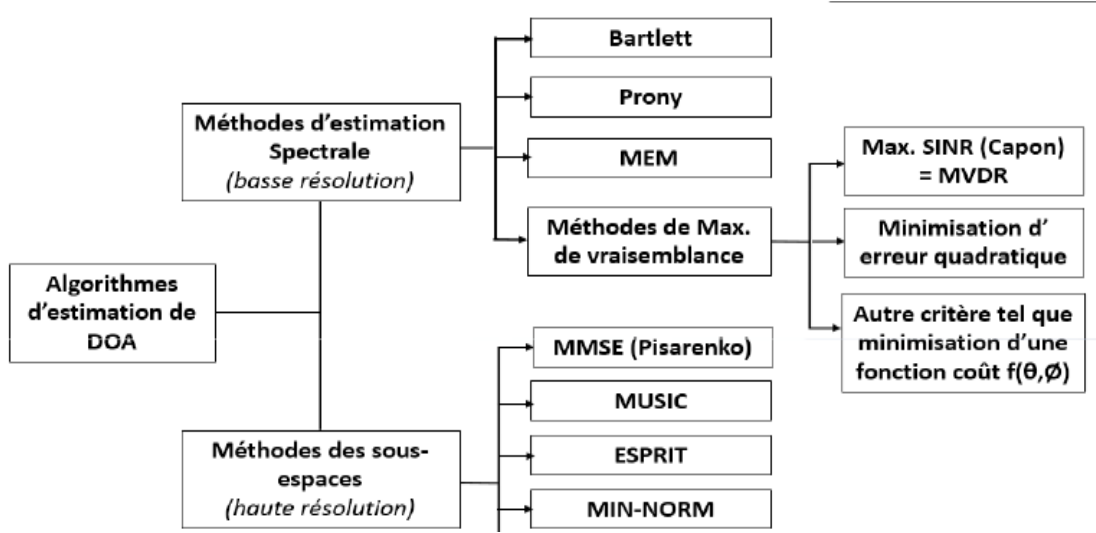


Figure 12. DDA estimation algorithms (TONYE, 2020)

### 3.2.2 Beamforming Algorithms

Beamforming algorithms, as explained above, have the role of focusing the radiation pattern in preferred directions and minimizing interference. In (<https://memoireonline.com/12/07/773/etude-cellules-rayonnantes-reseau-reflecteur2.png>), the signal in the absence of noise is:

$$X(t) = A(\theta, \phi) \cdot S \quad (18)$$

By replacing in  $Y = W^H X(t)$ , on obtient  $Y = W^H A(\theta, \phi) \cdot S$

We pose:

$$FR(\theta, \phi) = W^H A(\theta, \phi) \quad (19)$$

Its normalized value is:

$$FRN = \frac{FR(\theta, \phi)}{\max(FR)} \quad (20)$$

Where FR represents the network factor. It is used to calculate the radiation pattern when the weights of the different antenna elements are known. Having radiation suited to one's needs therefore amounts to adjusting the different values of the weights.

They can be subdivided into two:

#### 3.2.2.1 Fixed Conformers (Independent of User Data)

##### ▪ Conventional shaper

Also called “delay and sum beamformer” is the simplest of all shapers. If a signal from a known direction is chosen, then the main lobe of the array of radiating elements can be directed towards that direction. This is done by multiplying each element by a complex weight, corresponding to a delay, such that the signals coming from the desired direction on each element are combined and in phase.

$$w_i = e^{j(i-1)\tau} \quad (21)$$

Where  $i$  corresponds to the  $i$ th radiating element.

##### ▪ Lobe canceling conformator

The particularity of this shaper, compared to the conventional shaper, is that it also allows (assuming that we have information on the interferents), to cancel the interference lobes. It then maximizes the SIR ratio (Mubeen, Prasad,

& Rani, 2012):  $\frac{\text{Signal}}{\text{Interference}}$ .

### 3.2.2.2 Adaptive Conformers (dependent on user data)

#### ▪ MVDR Conformer

The lobe canceller shaper allows to maximize the SIR without taking into account the Gaussian noise. The MVDR shaper, on the other hand, maximizes the SNIR ratio:  $\frac{Signal}{Interférence+Bruit}$ .

To do this, in (Mubeen, Prasad, & Rani, 2012), the weight is :

$$w = \frac{R^{-1}s_0}{s_0^H R^{-1}s_0} \quad (22)$$

#### ▪ LMS Algorithm

This algorithm was introduced by Widrow and Hoff in 1959. According to (Hokam et al., 2016), the LMS algorithm can be described by the following 3 equations:

$$y(n) = w(n).x(n) \quad (23)$$

$$e(n) = d(n) - y(n) \quad (24)$$

$$w(n+1) = w(n) + \mu.x(n).e^*(n) \quad (25)$$

Where  $\mu$  represents the constant gain to control the adaptation rate,  $e(n)$  is the error between the desired signal and the output signal,  $y(n)$  is the output signal,  $x(n)$ , the signal input and  $d(n)$ , the desired signal.

#### ▪ RLS Algorithm

The convergence speed of the LMS algorithm depends on the eigenvalues of the correlation matrix. In a rapidly changing mobile environment that needs to produce a correlation matrix with a large number of eigenvalues, the LMS algorithm becomes slow. This problem is solved in the RLS algorithm by replacing  $\mu$  by the gain matrix  $R^{-1}(k)$  to the  $k$ th iteration, thus allowing us to update the equation (26):

$$w(k) = w(k-1) - R^{-1}(k)x(k)e^*(w(k-1)) \quad (26)$$

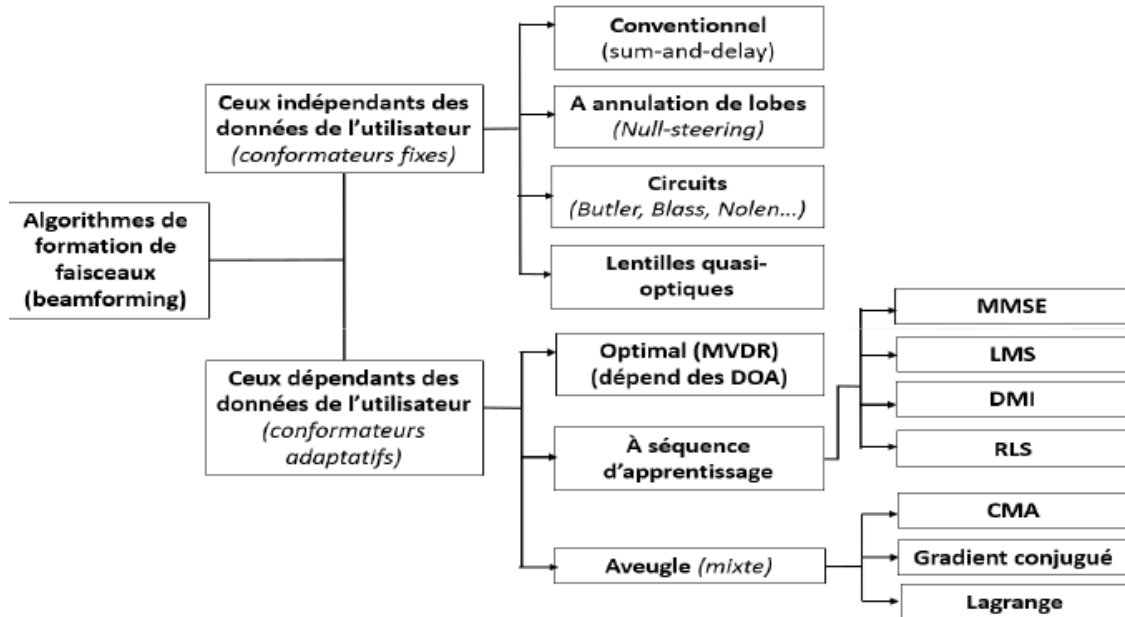


Figure 13. Beamforming algorithms (TONYE, 2020)

### 3.3 Implementation of Smart Antenna Algorithms

The technology of smart antennas has existed for years, many solutions have been developed to clearly illustrate their mechanism by implementing the algorithms mentioned above.

In (TONYE, 2020), S. KEPCHABE et E. TONYE have deployed an application on MATLAB 7.0. This application allows to:

- Illustrate the estimation of DDAs by implementing several analytical DDA algorithms (MUSIC, Capon, Bartlett, MEM, MMSE, Prony); and by genetic synthesis of these algorithms.
- Illustrate the phenomenon of beam radiation towards users while minimizing interference, by means of certain adaptive algorithms (DMI, Conventional, LMS, RLS, lobe canceller, CMA, MVDR) and by genetic synthesis of these algorithms.
- Evaluate and compare the simulation times of the different algorithms in the analytical method and in the genetic method.

The interface of said application is:

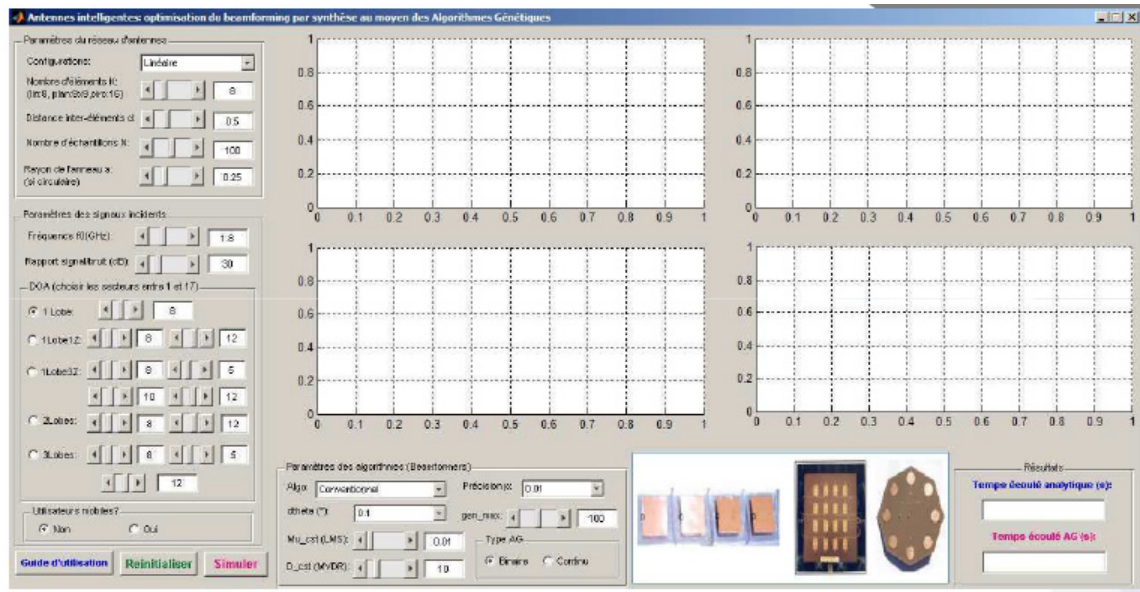


Figure 14. App interface (TONYE, 2020)

The focal point of this application is to simulate the performance of smart antennas by optimizing the analytical algorithms through the synthesis of other so-called “genetic” algorithms and to illustrate it by highlighting the different simulation times for one or more of them.

The results obtained are summarized in (TONYE, 2020) in the tables of Figures 15 and 16:

Estimateurs de DOA	Réseau linéaire				Réseau carré				Réseau circulaire			
	1Lobe	2Lobes	3Lobes	4Lobes	1Lobe	2Lobes	3Lobes	4Lobes	1Lobe	2Lobes	3Lobes	4Lobes
Bartlett	0,187	0,266	0,202	0,218	0,109	0,125	0,125	0,125	0,156	0,218	0,202	0,218
AG_Bartlett	0,780	0,796	0,780	0,795	1,716	1,747	1,701	1,701	0,780	0,795	0,795	0,811
Prony	0,234	0,250	0,218	0,203	2,850	2,880	2,917	2,918	0,218	0,202	0,187	0,202
AG_Prony	0,764	0,749	0,764	0,749	1,701	1,700	1,701	1,700	0,764	0,764	0,764	0,748
Capon	0,156	0,203	0,187	0,187	1,529	1,513	1,513	1,545	0,187	0,203	0,203	0,203
AG_Capon	0,765	0,765	0,764	0,764	1,700	1,716	1,700	1,716	0,749	0,764	0,780	0,764
MEM	0,171	0,172	0,156	0,172	0,110	0,125	0,109	0,125	0,187	0,187	0,172	0,156
AG_MEM	0,764	0,780	0,765	0,764	1,701	1,716	1,700	1,716	0,765	0,780	0,780	0,795
MMSE	0,188	0,172	0,171	0,172	0,125	0,125	0,109	0,140	0,234	0,171	0,188	0,187
AG_MMSE	0,764	0,780	0,766	0,764	1,701	1,700	1,701	1,716	0,780	0,796	0,765	0,780
MUSIC	0,359	0,218	0,234	0,250	0,781	0,343	0,265	0,250	0,156	0,172	0,156	0,172
AG_MUSIC	0,795	0,796	0,765	0,764	1,731	1,700	1,716	1,716	0,827	0,780	0,796	0,764
MIN-NORM	0,156	0,172	0,203	0,156	0,125	0,156	0,156	0,156	0,219	0,234	0,172	0,203
AG_MinNor	0,764	0,780	0,764	0,795	1,716	1,700	1,701	1,701	0,780	0,796	0,780	0,780

Figure 15. Elapsed times of beamforming by analytical methods and by genetic algorithms (50 to 100 times better) (TONYE, 2020)

Nombre de lobes souhaités	Méthodes analytiques	LINEAIRE			PLANAIRE			CIRCULAIRE		
		Temps écoulés Analytique	Temps écoulés AG	Performance	Temps écoulés Analytique	Temps écoulés AG	Performance	Temps écoulés Analytique	Temps écoulés AG	Performance
1 lobe	Conv.	0.312	0.406	≈	0.109	0.250	≈	0.187	0.062	≈
	MVDR	6.193	0.406	17 fois plus petit	11.091	0.265		6.802	0.062	
	LMS	6.989	0.406		10.671	0.265		7.519	0.062	
1 lobe 1 zero	MVDR	5.897	0.047	125 fois plus petit	11.185	0.265	42 fois plus petit	6.864	0.063	12 fois plus petit
	LMS	5.944	0.047		11.341	0.265		7.582	0.063	
1 lobe 3 zeros	MVDR	5.928	0.047		11.326	0.265		6.927	0.062	
	LMS	5.897	0.047		10.343	0.249		7.519	0.063	
2 lobes	MVDR	6.147	0.046	132 fois plus petit	11.061	0.250		6.802	0.062	
	LMS	6.131	0.046		10.577	0.265		7.379	0.062	
3 lobes	MVDR	6.193	0.047		11.154	0.265		6.740	0.062	
	LMS	6.147	0.047		10.483	0.250		7.317	0.062	

Figure 16. Beamforming time per synthesis using genetic algorithms for N=100 (TONYE, 2020)

## 4. Tools and Methods

### 4.1 Tools

For the design of the application, physically, we used an HP brand computer whose processor is AMD Athlon with 2GB of RAM. In software, we used the MATLAB R2016a application.

Specifically, we used the MATLAB GUI tool. This tool makes it possible to deploy graphic-user spaces whose interface can be designed according to each user. To do this, enter the word: guide in the “Command Window”. Once entered, the following window opens:

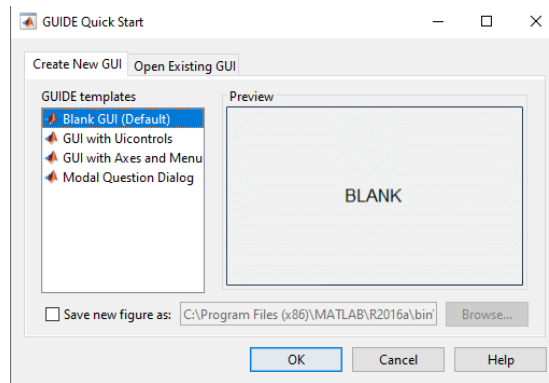


Figure 17. Opening MATLAB GUI

Select: Create New GUI, choose the path and click OK. We obtain:

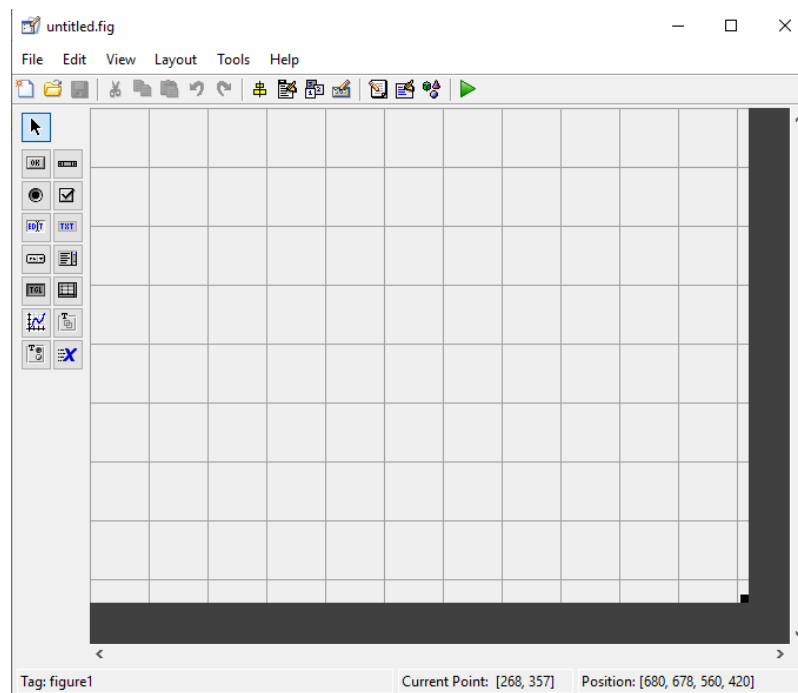


Figure 18. Blank MATLAB GUI File

#### 4.2 Flowchart of the Methodological Steps

The methodological steps of the graphical user interface of our application are summarized in the following UML sequence diagram:



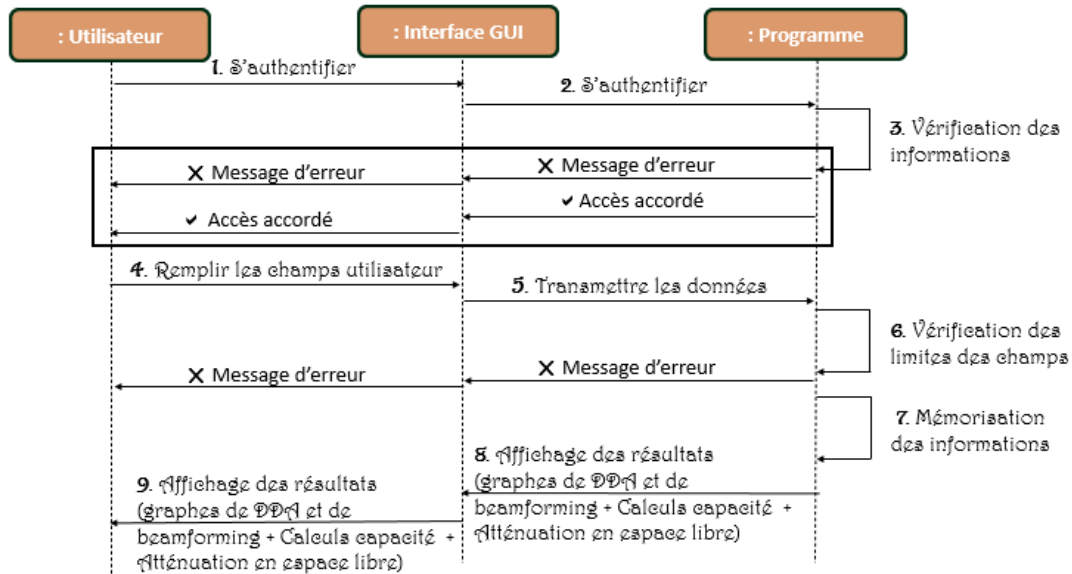


Figure 19. Sequence diagram of small cell performance

This diagram can be summarized in four main steps:

- Authentication at the interface

Once the user is authenticated with the correct credentials at the login page, access to the interface is granted.

- Fields filled in by the user

Once the interface is open, the user has a certain number of fields to fill in corresponding to the input parameters. At the program level, it will be checked that the user does not enter incorrect data. If not, it will receive an error message indicating the correct data value range.

- Display of results

The input parameters being saved in the program, the latter will start to give the different results: curves and calculation results.

#### 4.3 Architecture de l'application

The application architecture is detailed in the following figure:

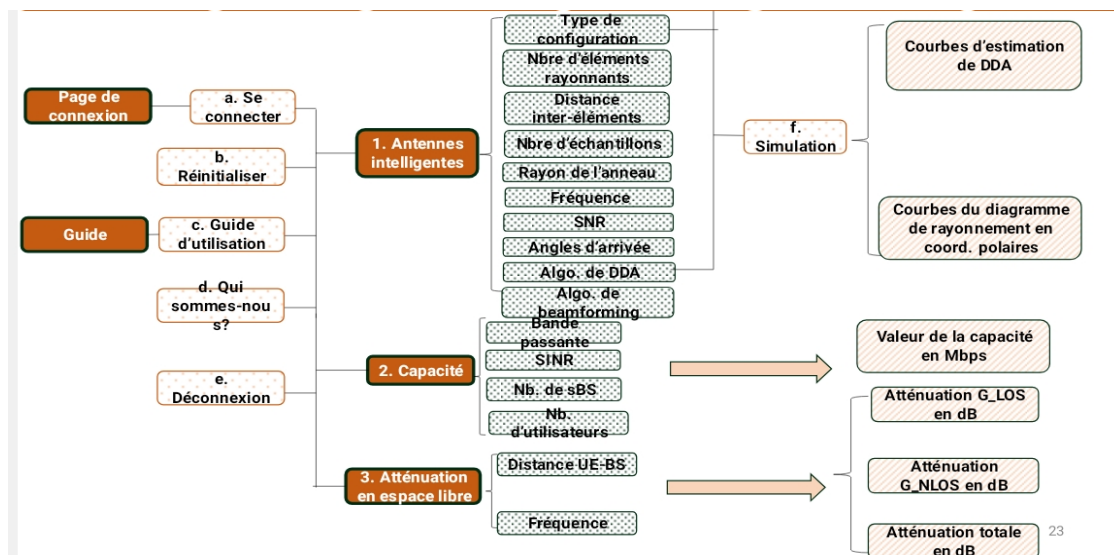


Figure 20. Application architecture

Tag :



This type of frame is used for application buttons.



This type of framework is used for results.



This type of frame is used for the different pages of the application and the three parts of the interface page.



This type of frame is used for the parameters to be entered in the interface page.

#### 4.4 Development

Once the visual aspect of the graphical user interface of our application has been designed, MATLAB automatically generates the skeleton code of the application. It is up to us to add lines of code to obtain results in line with the objectives set.

### 5. Scenarios, Results and Discussions

#### 5.1 Overview of the App



Figure 21. Graphical interface of the application divided into 3 parts

Our interface is divided into three main parts as shown in Figure 36:

- 1) Smart antennas
- 2) The densification of the network by its capacity
- 3) Signal attenuation in free space in a micro cell

#### Structure

The application that was deployed as part of this work consists of three pages:

☞ The login page

*It allows a user to authenticate to access the application. Here, the identifiers (Email + Password) are unique. It is from this page that you can access the interface of the application. If the credentials are not correct, the application will return an error message: "The email and/or password entered is (are) invalid".*

☞ The graphical user interface of the application

It is the heart of the application, because it is from it that the user will be able to enter input parameters and have output results.

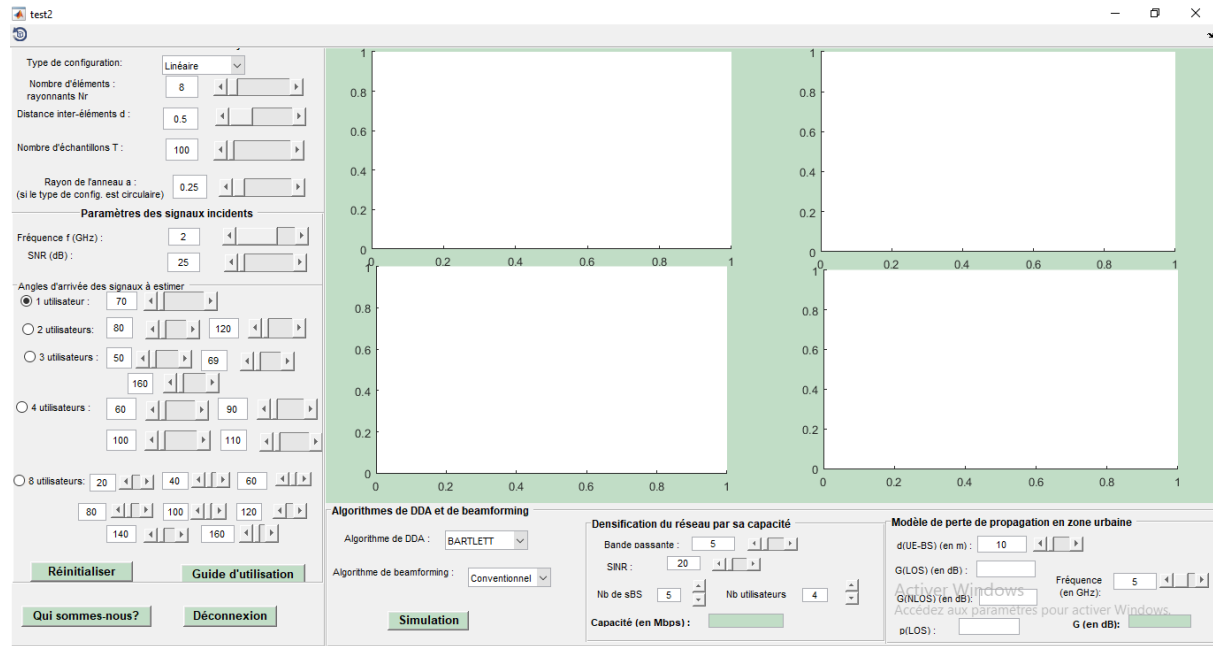


Figure 22. The application interface page

#### The user guide

It provides information on the information of the input parameters, the limits of the values of these parameters and their possible impact on the results. In addition, this guide provides some calculation formulas. It is accessed by the user guide button on the interface.

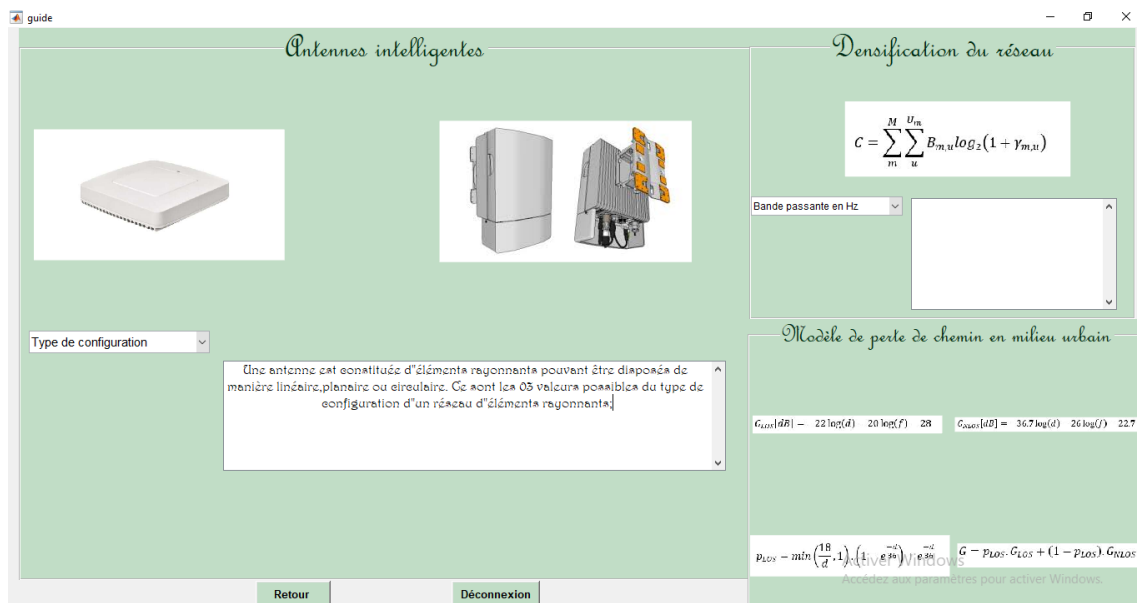


Figure 23. The application user guide page

From this page, you can return to the application interface or disconnect from the application.

### 5.2 Smart Antenna Results

To clearly illustrate the mechanism of smart antennas, we have chosen some DDA estimation and beamforming

algorithms. The source codes used are open-source and we took them from <https://memoireonline.com/12/07/773/etude-cellules-rayonnantes-reseau-reflecteur2.png>.

The parameters used to show the performance of the smart antennas, the corresponding variables used in the program and the ranges of values are:

☞ The number of radiating elements present in the antenna:  $N_r$

In (Cooper, 2003), an antenna consists of 4 to 12 radiating elements. With new technological challenges including increased capacity, 5G and smart antennas, this number has increased significantly and may increase further in the coming years. This is the reason why  $N_r$  ranges from 8 to 50 radiating elements. The type of configuration can take three values representing the arrangement of the radiating elements inside the antenna: linear, planar, circular.

☞ The distance between the radiating elements:  $d$

This distance, for the dipoles, is evaluated at  $0.5\lambda$ . Thus, the values of  $d$  are between  $0.2\lambda$  and  $1\lambda$ .

☞ The number of samples:  $T$

It represents the number of observations under which the signals arrive on the network of radiating elements.  $T$  ranges from 1 to 100.

☞ The radius of the ring:  $a$  (if the type of configuration is circular)

Values range from 0.25 m to 2 m.

☞ The frequency:  $f$

As the radius of the cells is reduced, consequently, the frequency of the signal is of the order of GHz. Thus,  $f$  goes from 2 to 6 GHz.

☞ SNR ratio in dB

It goes from 3 to 70 dB, because it is estimated that a value above 70 dB, in free space, is utopian.

☞ DOA angles of arrival ranging from 1 to  $180^\circ$ .

The angles of arrival of the signals depend on the number of user equipments which send signals in the direction of the antenna. In the application, one can have: 1 user, 2 users, 3 users, 4 users and 8 users.

☞ The DDA estimation algorithm

We deployed seven DDA estimation algorithms that take into account all the above parameters: Bartlett, Prony, MEM, MMSE, MINNORM, MUSIC and CAPON.

Below, is presented a part of the codes highlighting the role of the input parameters in the determination of the pseudo-spectrum.

```

2252 - if get(handles.lobel,'Value')==1
2253 -     doa=doal/180*pi; %Convertir l'angle d'arrivée en radians
2254 -     w=pi/3;
2255 -     L=length(doa);
2256 -     A=zeros(Nr,L); %initialiser la matrice des vecteurs directionnels des sources
2257 - for i=1:L
2258 -     A(:,i)=transpose(exp(-1j*k*d1*cos(doa(i))*(0:Nr-1))); %Remplir la matrice des vecteurs directionnels des sources
2259 - end
2260 - S=2*exp(1j*(w*(1:T))); % Le vecteur des enveloppes complexes des sources
2261 -
2262 - X=A*S; % Le signal sans bruit
2263 - X=X+awgn(X,snr); %Le signal arrivant au niveau de l'antenne avec le bruit additif gaussien
2264 -
2265 - Rxx=X*X'/T; % La matrice de covariance

```

Figure 24. Part of the code highlighting the determination of DDA (1/3)

As illustrated in Figure 43, we will first determine the matrix  $A$  of the directional vectors of the sources.  $A$  is the transpose of the elements  $a(\theta_k)$

$$A = [a(\theta_1), a(\theta_2), \dots, a(\theta_D)]^T$$

Où  $a_n(\theta_k) = \exp(-j(n-1) * k * d * \cos(\theta_k))$  (n represent the nth radiating element).

By assuming  $\varphi_k = k * \cos(\theta_k)$ , we obtain :

$$A = \begin{bmatrix} 1 & 1 & \dots & 1 \\ e^{-\varphi_1} & e^{-\varphi_2} & \dots & e^{-\varphi_D} \\ \vdots & \vdots & \ddots & \vdots \\ e^{-(Nr-1)\varphi_1} & e^{-(Nr-1)\varphi_2} & \dots & e^{-(Nr-1)\varphi_D} \end{bmatrix} \quad (28)$$

Subsequently, we will determine the source signal.

The source signal S can be determined by the formula:

$$S = 2 * \exp(j * w * (T - 1)) \quad (29)$$

Where  $w = \frac{2\pi c}{\lambda}$

Thus, for each additional observation T of the signal, there will be an additional precision on the source signal.

Next, we will determine the noise which is considered here as white Gaussian noise.

As a result, and from equations (25) and (26), we obtain the matrix  $X = A \cdot S + N$ .

The covariance matrix is determined by:

$$R_{XX} = X * X^T \quad (30)$$

```

2272 %algo Bartlett début
2273 - Pb = zeros(1,theta_size(2)); %Initialiser la puissance du pseudo spectre de Bartlett
2274 - for kk = 1:theta_size(2)
2275 -     A = transpose(exp(-j*k*d1*(0:Nr-1)*cos(theta(kk))));
2276 -     Pb(kk) = abs(A'*Rxx*A)/Nr^2; %Déterminer la puissance de Bartlett
2277 - end
2278 - PbdB = 10*log10(Pb/max(Pb)); %Déterminer la puissance de Bartlett en dB
2279 %algo Barlett : fin
2280
2281 %algo Prony début
2282 - u = zeros(Nr,1);
2283 - u(round(L/2)) = 1;
2284 - Pp = zeros(1,theta_size(2)); %Initialiser la puissance du pseudo spectre de Prony
2285 - for kk = 1:theta_size(2)
2286 -     A = transpose(exp(-j*k*d1*(0:Nr-1)*cos(theta(kk))));
2287 -     Pp(kk) = (abs(u'*inv(Rxx)*u)) / ((abs(u'*inv(Rxx)*A))^2); %Déterminer la puissance de Prony
2288 - end
2289 - PpdB = 10*log10(Pp/max(Pp)); %Déterminer la puissance de Prony en dB
2290 % PRONY: fin

```

Figure 25. Part of the source code highlighting the determination of DDA (2/3)

Figure 25 is a continuation of Figure 24. Indeed, after determination of the covariance matrix  $R_{xx}$ , the next step is the determination of the power pseudo-spectrum which differs according to the implemented algorithm. So, using the BARTLETT algorithm, this pseudo-spectrum is evaluated at:

$$P_B = \frac{|A * R_{XX} * A^T|}{N_r^2} \quad (31)$$

From this formula follows:

$$P_B(dB) = 10 * 10 \log \frac{P_B}{\max(P_B)} \quad (32)$$

Once the equation (29) is drawn, the power peaks correspond to the directions estimated by DDA by the Bartlett algorithm.

☞ The beamforming algorithm

Here, we could only deploy the conventional algorithm which also uses the same input parameters as the DDA

estimation algorithms.

```

2356 -         dtheta =0.1;
2357 -         kd =2*pi*d;
2358 -         theta_all_deg = [doal]';
2359 -         theta_all =theta_all_deg*(pi/180);
2360 -         theta_degr = (0:dtheta:180-dtheta);
2361 -         theta =theta_degr*(pi/180);
2362 -         m= (1:1:Nr)';
2363 -         a = exp(1i*kd*(m-1)*cos(theta)); %Déterminer la matrice des vecteurs directionnels des sources
2364 -         w = (1/Nr)*exp(1i*kd*(m-1)*cos(theta_all)); %Déterminer la matrice des poids
2365 -         %Array factor (AF)
2366 -         AF = w'*a; %Déterminer le facteur de réseau
2367 -
2368 -         %Normalized array factor (NAF)
2369 -         epsilon =1E-100;
2370 -         AF= AF+epsilon;
2371 -         NAF =AF/max(AF); %Déterminer le facteur de réseau normalisé

```

Figure 26. Part of the code that highlights beamforming (3/3)

Having determined the matrix of direction vectors A, here it is a matter of finding the weights to adjust w:

$$w = \frac{1}{N_r} e^{(j*2*\pi*d*(Nr-1)*\cos(\theta_k))} \quad (33)$$

From (25) and (30), we get the network factor:

$$AF = A * w \quad (34)$$

Subsequently, the network factor AF is plotted, which corresponds to the radiation pattern of the antenna.

#### 5.2.1 Network Densification Through Capacity

As explained above, the capacity in a telephone network depends on:

- ☞ The bandwidth in MHz whose values range from 5 MHz to 100 MHz.
- ☞ The SINR whose values oscillate between 1 and 45 dB given that the interferences reduce the value of the SNR evaluated above.
- ☞ The number of small cells which goes from 1 to 10.
- ☞ The number of users which ranges from 1 to 10. These values were arbitrarily chosen by us.

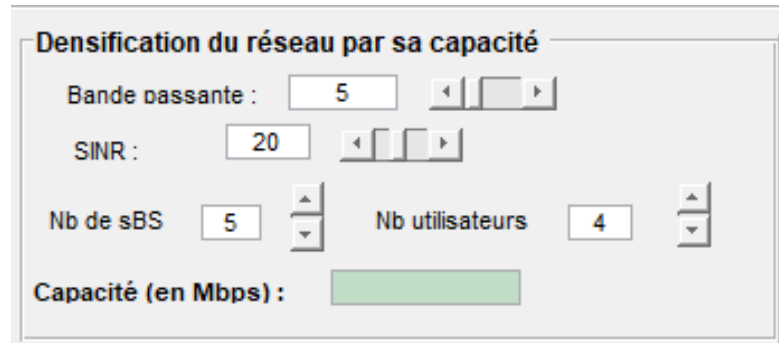


Figure 27. Application interface (capacity calculation in a heterogeneous network)

#### 5.2.2 Signal Attenuation in Free Space

According to the formula for free space attenuation in a microcell, it depends on:

☞ The frequency

Its value fluctuates between 2 GHz and 6 GHz.

☞ The distance between user equipment and small cell

It extends from 10 m to 2000 m representing the minimum and maximum small cell radii.

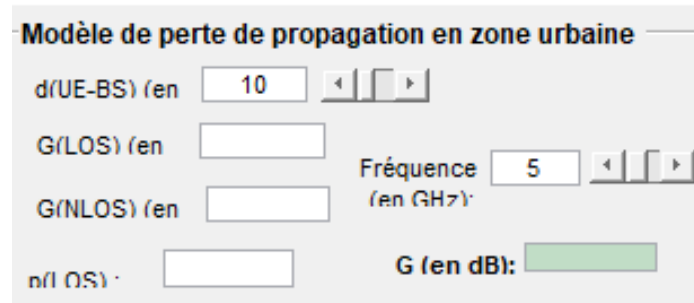


Figure 28. Application Interface (Urban Free Space Signal Attenuation in a Microcell)

### 5.2.3 Estimation of User Directions

As explained above, smart antennas must first estimate the directions of users in order to radiate only in those directions.

We used seven DDA estimation algorithms in order to be able to compare them and deduce the most efficient(s). The chosen scenario is consistent with that used in (TONYE, 2020). We will therefore analyze the results obtained with this scenario and compare them with the results obtained in (TONYE, 2020).

**Scenario:** Consider a linear network of 8 radiating elements regularly spaced by a distance  $d=0.5\lambda$  on which arrive signals of frequency  $f=2$  GHz, of SNR=30 dB coming from the directions  $50^\circ$ ,  $80^\circ$  and  $120^\circ$ .

Just like in (Hokam et al., 2016), we used seven DDA estimation algorithms: Bartlett, Prony, MEM, MMSE, MIN-NORM, MUSIC and Capon.  $50^\circ$ ,  $80^\circ$  and  $120^\circ$ .

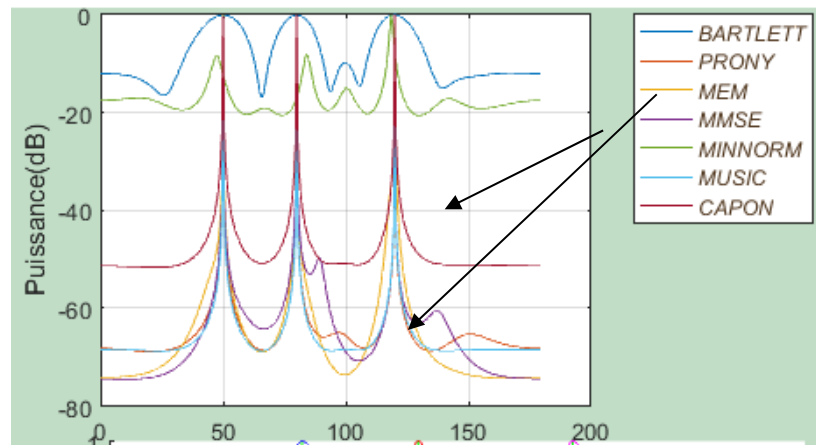


Figure 29. DDA estimation algorithms on the same graph

Various criteria will allow us to determine the best performing algorithm(s):

- ☞ The accuracy of the estimation of angles  $50^\circ$ ,  $80^\circ$  and  $120^\circ$
- ☞ The observation of three peaks in the directions  $50^\circ$ ,  $80^\circ$  and  $120^\circ$
- ☞ These peaks must be of the highest possible powers.

After analyzing these criteria, it appears that the best performing DDA estimation algorithms are: MUSIC and Capon. So we decided to isolate the performance of these two algorithms for better visibility:



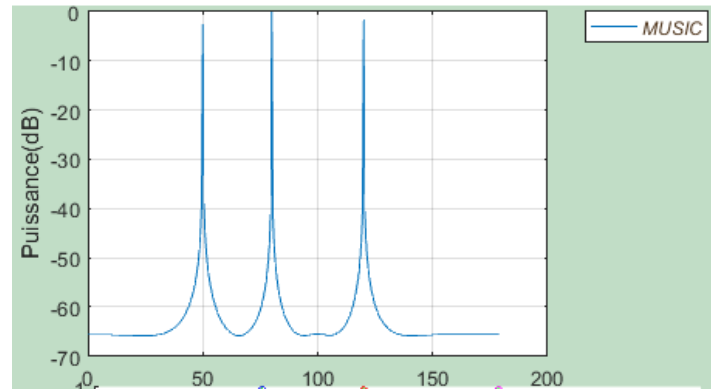


Figure 30. Algorithme MUSIC estimant les directions 50°, 80° et 120°

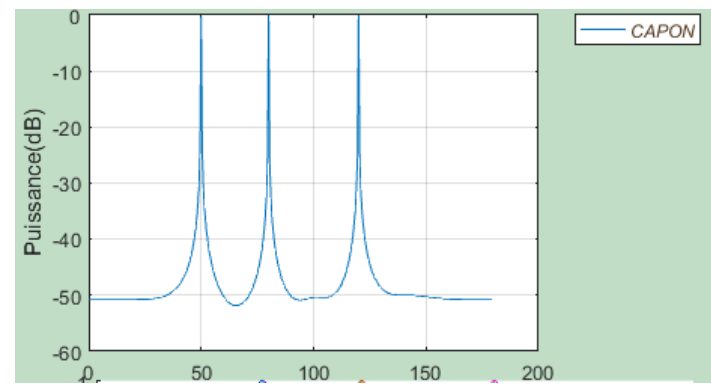


Figure 31. Capon algorithm estimating 50°, 80° and 120° directions

In Elimam and Remana (2013), the authors obtained:

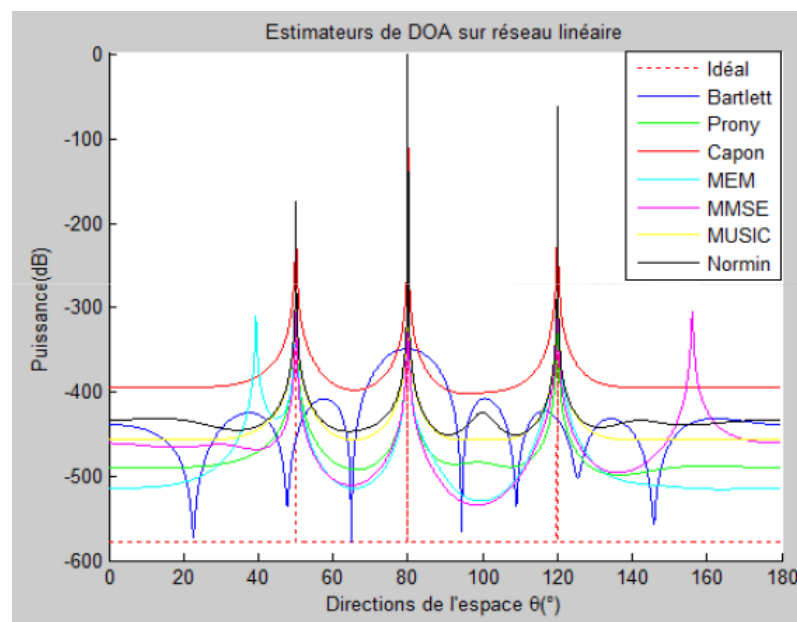


Figure 32. DDA estimation algorithms estimating the 50°, 80° and 120° directions on the same graph obtained in the literature (Elimam & Remana, 2013)

Note that it is the MIN-NORM (Black), MUSIC (yellow) and Capon (Red) algorithms that best estimate the directions  $50^\circ$ ,  $80^\circ$  and  $120^\circ$ . Compared to our application, the MUSIC and Capon algorithms are among those that best estimate the DDA of signals from users, with the only difference that the MIN-NORM algorithm has been added.

#### 5.2.4 Radiation in Estimated Directions

Once the angles of the users are known, the smart antenna should radiate in those directions in such a way that the beams are directed towards the users and interference is kept to a minimum.

**Scenario:** Consider a planar array of regularly spaced radiating elements with a distance  $d=0.5\lambda$ . 2 GHz frequency signals, whose SNR is 30 dB from eight directions (users)  $20^\circ$ ,  $40^\circ$ ,  $60^\circ$ ,  $80^\circ$ ,  $100^\circ$ ,  $120^\circ$ ,  $140^\circ$  and  $160^\circ$  arrive on this network of radiating elements.

We decided to make a comparison of the results obtained according to the number of radiating elements present in the planar array and to deduce the impact on the efficiency of the radiation of the antennas.

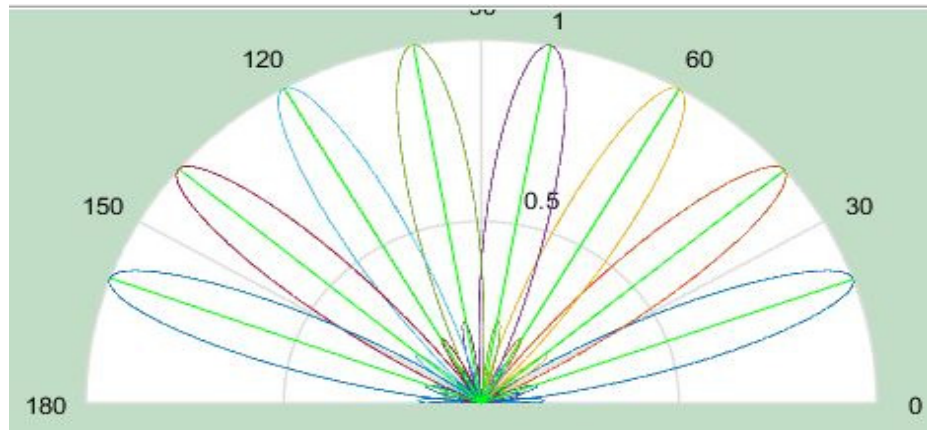


Figure 33. Diagramme de rayonnement lorsque le nombre d'éléments rayonnants est  $8 \times 8$

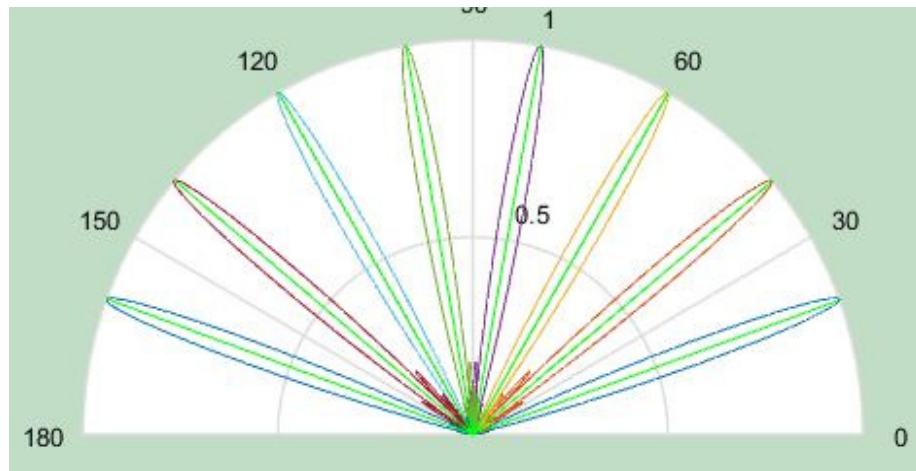


Figure 34. Radiation diagram when the number of radiating elements is  $22 \times 22$

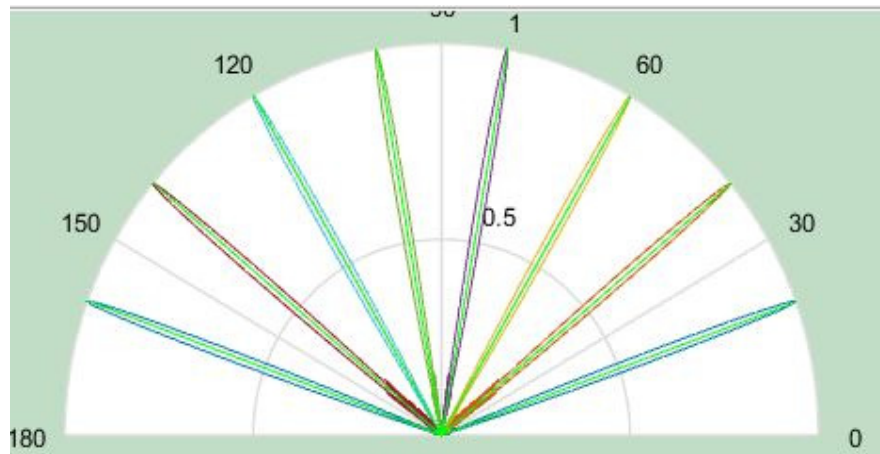


Figure 35. Radiation diagram when the number of radiating elements is 50\*50

These graphs show the radiation patterns of a smart antenna. On these graphs, there are main lobes of maximum power, directed in the directions of the users and secondary lobes of lower powers representing interference.

It can be seen that the greater the number of radiating elements, the more directional is the radiation pattern in the desired directions and the less interference there is. It can be seen that the greater the number of radiating elements in the antenna, the stronger the power of the radiation pattern in the desired directions and the less the interference.

#### 5.2.5 Network Densification Throughout Capacity

In this part, it is a question of showing how the problem of slow connection speeds can be solved by deploying small cells in Cameroon. To illustrate this, we carried out a connection speed test with a smartphone, in 4G with a mobile operator from Cameroon.



**ZONE ADSL**

🏠 > Test de débit 4G > Résultats

## Résultats test de débit

le 27/06/2022 à 10h50 près de Douala ()

Renseignez votre adresse pour comparer votre débit à celui des habitants de votre ville.

🔍 Saisissez votre adresse

**Préciser le test**

**orange**

⬇️ **4 Mb/s**  
en descendant / download

⬆️ **6,1 Mb/s**  
en montant / upload

**24 ms**  
ping / latence

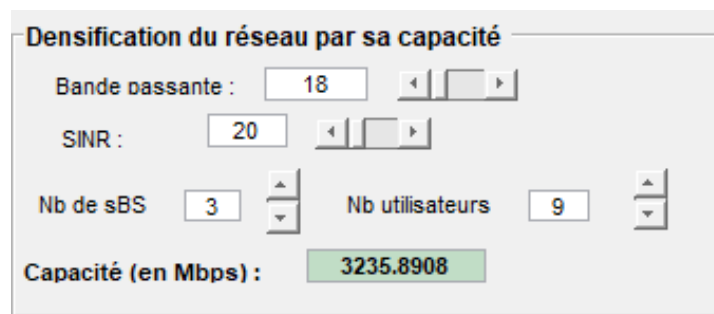
📞

Figure 36. 4G speed test

In Figure 36, we can see as results that the connection rate at that time oscillates between 4 Mbps (downlink rate) and 6.1 Mbps (uplink rate). Also, the latency is 24ms which is huge. Indeed, latency refers to the time taken by a data packet to leave from point A to point B. Therefore, 24 ms is huge in terms of latency knowing that in 5G, we aspire to a latency of 1ms.

With our application, we decided to calculate the throughput with the deployment of small cells.

**Scenario:** We are in a heterogeneous network in which the bandwidth is 18 MHz and an SINR of 20 Db.



**Densification du réseau par sa capacité**

Bande passante : 18

SINR : 20

Nb de sBS : 3

Nb utilisateurs : 9

Capacité (en Mbps) : 3235.8908

Figure 37. Capacity calculation for 3 small cells and 9 users present at the same time in the heterogeneous network

We get a boosted capacity **up to about 3 Gbps**.

**Densification du réseau par sa capacité**

Bande passante : 18

SINR : 20

Nb de sBS : 4

Nb utilisateurs : 4

**Capacité (en Mbps) : 1917.5649**

Figure 38. Capacity calculation for 4 small cells and 4 users present at the same time in the heterogeneous network

As shown in Figure 41, the capacity in a heterogeneous network where there are 4 small cells and 4 users at the same time is **1.9 Gbps**.

In a more summary way, we have produced a 3D figure showing the capacity according to the number of users and the number of small cells, for a bandwidth of 18 MHz and an SINR of 20 dB.

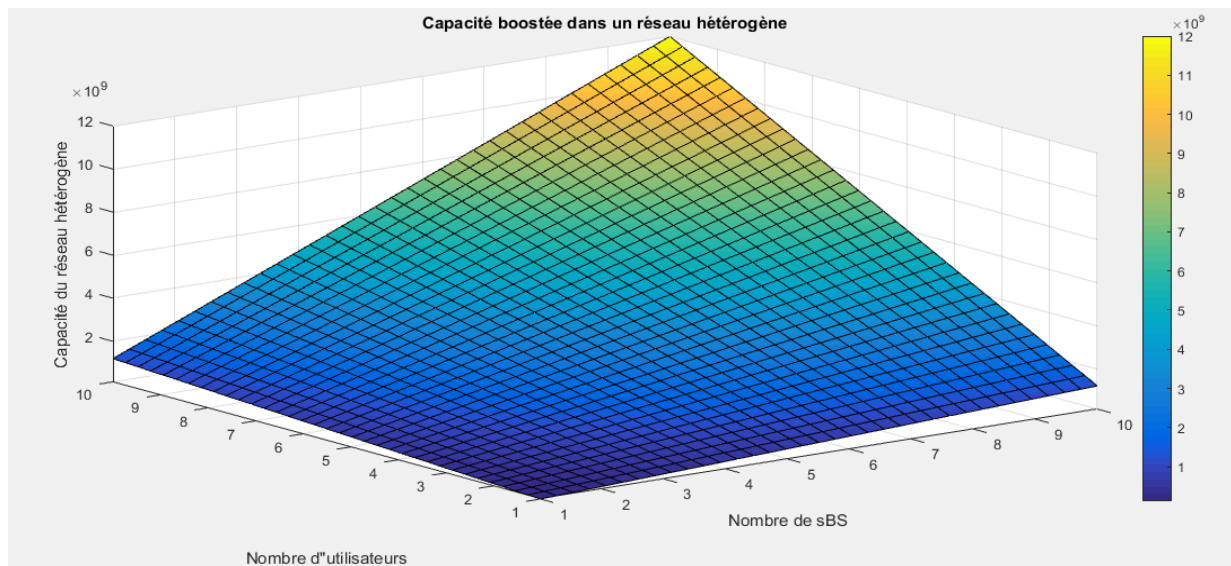


Figure 39. Capacity in bps according to the number of users and a number of small cells for a BP of 18 MHz and a SINR of 20 dB

### 5.3 Results Attenuation of the Signal in free Space in An Urban Environment in a Microcell

To evaluate the attenuation in free space in a microcell, it is necessary to pre-evaluate the attenuation in the LOS environment and the attenuation in the NLOS environment.

**Scenario:** We are in a microcell whose signal is of frequency  $f=5$  GHz.

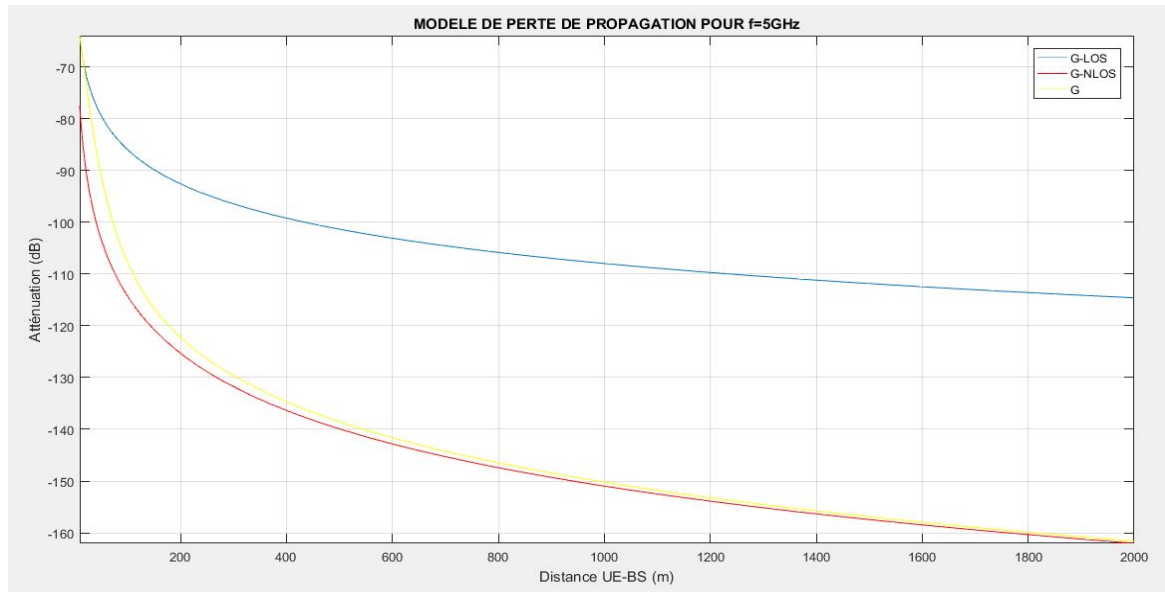


Figure 40. Signal attenuation in free space in LOS area, NLOS area and total attenuation as a function of user-small cells distance

Note that for small distances  $d$  ranging from 10 m to about 40 m, the total attenuation (yellow) is greater than -80 dB and almost coincides with the LOS attenuation (blue); because, between the user and the small cell, there are very few obstacles.

On the other hand, for larger distances  $d$  ranging from 600 m to 2000 m, the total attenuation is less than -140 dB and almost confounded with the NLOS attenuation (red); because, between the user and the small cell, there are many obstacles (buildings, shrubs).

In order to confirm the analyzes made above, we will proceed by calculation:

Figure 41. Calculation of signal attenuation in a microcell for a frequency of 5 GHz and  $d(\text{UE-SC}) = 10\text{m}$

For a distance of 10 m between the user and the small cell, the total attenuation is very close to the attenuation in free space or even equal.

**Modèle de perte de propagation en zone urbaine**

d(UE-BS) (en m) : 600

G(LOS) (en dB) : -103.0987

G(NLOS) (en dB) : -142.8314

p(LOS) : 0.03

Fréquence (en GHz) : 5

G (en dB) : -141.6394

Figure 42. Calculation of signal attenuation in a microcell for a frequency of 5 GHz and  $d(\text{UE-SC}) = 600\text{m}$

For a distance of 600 m between the user and the small cell, it is clearly seen that the total attenuation  $G$  tends towards the attenuation in the NLOS zone.

By knowing the impact of the distance between the user and the small cell on the attenuation of the signal (and therefore on the performance of the small cell), this will make it possible to take this into account, by establishing the minimum distances between the small cells during the sizing study prior to their deployment.

## 6. Conclusion and Perspectives

At the end of this work, which offers an efficient and sustainable solution for the deployment of small cells in mobile networks, we have proposed smart antennas instead of conventional antennas. This was followed by the design of an application under MATLAB which makes it possible to illustrate the performance of small cells in general: the capacity of the network boosted with their deployment, the attenuation of the signal taking into account the distance between the user and the small cell; and, in particular, the mechanism of smart antennas by means of algorithms allowing this type of antennas to radiate in privileged directions at specific times.

However, the app has some limitations. Indeed, small cells with smart antennas are an effective solution, but what would improve their effectiveness is the response time between the request from a user and the radiation of electromagnetic waves in his direction. This time can be optimized by calculating the simulation times of the different algorithms used, analyzing them and comparing them for better responsiveness of small cells with smart antennas. Moreover, regarding the different algorithms used for the radiation itself, we only used the conventional algorithm. Finally, we believe that it is possible to directly implement the intelligence of the antennas to be integrated into the small cells by means of artificial intelligence.

## References

- Claussen, H., Lopez-Perez, D., Ho, L., Razavi, R., & Kucera, S. (2017). *Small cell networks: deployment, management, and optimization*. John Wiley & Sons. <https://doi.org/10.1002/9781119307600>
- Contrôles Essais Mesures. (2022). Test de 5G Small Cell (petites cellules 5G) opérant aux fréquences millimétriques. Retrieved July 15, 2022, <https://www.google.com/amp/s/www.controles-essais-mesures.fr/mesures/0015767-test-de-5g-small-cell-petites-cellules-5g-operant-aux-frequences-millimetriques/amp/>
- Cooper, M. (2003). Les antennes intelligentes. *Pour la science*, (312), 72-78.
- Elimam, M., & Remana, F. (2013). Estimation des directions d'arrivée DoA en utilisant une rangée d'antennes linéaire par les méthodes: BEAMFORMER, CAPON et PREDICTION LINEAIRE. Mémoire de projet de fin d'études pour l'obtention du diplôme de master en Aéronautique, Institut d'Aéronautique et des Etudes spatiales (BLIDA), pp 16, 2013.
- GSM Association. (2016). GSMA Improving Wireless connectivity through small cell deployment. Retrieved from GSM Association [https://www.google.com/url?sa=i&rct=j&q=&esrc=s&source=web&cd=&ved=0CAIQw7AJahcKEwiAgt6p\\_J7\\_AhUAAAAAHQAAAAAQBBQ&url=https%3A%2F%2Fwww.gsma.com%2Fpublicpolicy%2Fwp-content%2Fuploads%2F2016%2F12%2FGSMA\\_Small\\_Cell\\_Deployment\\_Booklet.pdf&psig=AOvVaw2-M2dW\\_cBWlj338x1Hbx1&ust=1685602313702903](https://www.google.com/url?sa=i&rct=j&q=&esrc=s&source=web&cd=&ved=0CAIQw7AJahcKEwiAgt6p_J7_AhUAAAAAHQAAAAAQBBQ&url=https%3A%2F%2Fwww.gsma.com%2Fpublicpolicy%2Fwp-content%2Fuploads%2F2016%2F12%2FGSMA_Small_Cell_Deployment_Booklet.pdf&psig=AOvVaw2-M2dW_cBWlj338x1Hbx1&ust=1685602313702903)
- Hokam, S., Dandekar, A., Tiwari, A., & Sheikh, G. (2016). An overview of LMS adaptive beamforming algorithm for smart antenna. *International Journal of Advanced Research in Electrical, Electronics and Instrumentation*



*Engineering*, 5, Janvier 2016.

- Issakov, V. (2016). Highly-Integrated Millimetre-Wave Systems for Small-Cell Backhaul Communication Applications, the *11th European Microwave Integrated Circuits Conference* (Huawei Technologies CO., LTD), 2016, page 5.
- Kamil, A. A., Ismail, M. M., & Bashar, B. S. (2021). Comparative and analysis of evaluation of several direction of arrival estimation methods. *TELKOMNIKA (Telecommunication Computing Electronics and Control)*, 19(5), 1724-1734. <https://doi.org/10.12928/telkomnika.v19i5.18744>
- Les bénéfices de la 5G. Retrieved June 15, 2022, from <https://radio-waves.orange.com/fr/reseaux-et-antennes/5g/les-benefices-de-la-5g/>
- Mubeen, S., Prasad, A. M., & Rani, D. A. J. (2012). Smart antennas it's beam forming and doa. *International Journal of Scientific and Research Publications*, 2(5), 1-5.
- Naceur, A., & Merahi, B. (2012). L'estimation de l'Angle d'Arrivée et la Formation de Voie par un Système à Antenne Intelligente. *International Congress on telecommunication and application*, University of A.MIRA Bejaia, Algeria, APRIL 2012.
- Par Ando, R. (2021). 6G: guide complet sur la sixième génération de réseau sans fil. Retrieved July 15, 2022, from <https://www.google.com/amp/s/www.objetconnecte.com/6g-guide-complet/amp/>
- Retrieved February 19, 2023, from [https://www.researchgate.net/publication/281460203\\_Simulation\\_des\\_performances\\_des\\_antennes\\_intelligentes\\_par\\_approches\\_analytiques](https://www.researchgate.net/publication/281460203_Simulation_des_performances_des_antennes_intelligentes_par_approches_analytiques)
- Retrieved July 15, 2022, from <https://www.google.com/amp/s/www.lesechos.fr/amp/1357263> (consulté le 15 juillet 2022)
- Retrieved June 15, 2022, from <https://encrypted-tbn0.gstatic.com/images?q=tbn:ANd9GcQuL-DMFyYtCpOrGRToLkYNP0ckLeCqx36-5g&usqp=CAU>
- Retrieved June 27, 2022, from <https://cdn.sketchbubble.com/pub/media/catalog/product/optimized1/a/9/a9c208093dc77b45f6c3518a311fac25167e840ef765f526f567b06184fd69f8/line-of-sight-model-mc-slide1.png>
- Retrieved June, 2022, from <https://memoireonline.com/12/07/773/etude-cellules-rayonnantes-reseau-reflecteur2.png>
- Retrieved June, 2022, from <https://www.researchgate.net/profile/Subha-Ghosh/publication/337432350/figure/fig1/AS:962228639510561@1606424593740/Small-cell-clustering-under-microcell-base-station.png>
- Retrieved March 28, 2022, from <https://blogs.univ-poitiers.fr/f-launay/files/2021/01/figure11.png>
- Shannon, C. E. (1949). Communication in the presence of noise. *Proc. Inst. Radio Eng.*, 37(1), 10-21. <https://doi.org/10.1109/JRPROC.1949.232969>
- TONYE, E. (2020). Antennes intelligentes: analyse des performances par l'exemple. Generis publishing, mars 2020
- Tonye, E., & Kepchabe, S. (2023). Simulation des performances des antennes intelligentes par approches analytiques.
- Tout savoir sur les antennes 5G. Retrieved April 3, 2022, from <https://blog.ariase.com/mobile/dossiers/antennes-5G>
- Webb, W. (Ed.). (2007). *Wireless communications: The future*. John Wiley & Sons. <https://doi.org/10.1002/9780470065129>

## Copyrights

Copyright for this article is retained by the author(s), with first publication rights granted to the journal.

This is an open-access article distributed under the terms and conditions of the Creative Commons Attribution license (<http://creativecommons.org/licenses/by/4.0/>).